

Patient-Specific Skeletal Muscle Fiber Modeling from Structure Tensor Field of Clinical CT Images

Yoshito Otake¹(✉), Futoshi Yokota¹, Norio Fukuda¹, Masaki Takao²,
Shu Takagi³, Naoto Yamamura³, Lauren J. O'Donnell⁴, Carl-Fredrik Westin⁴,
Nobuhiko Sugano³, and Yoshinobu Sato¹

¹ Graduate School of Information Science,
Nara Institute of Science and Technology, Ikoma, Japan
otake@is.naist.jp

² Graduate School of Medicine, Osaka University, Suita, Japan

³ Department of Mechanical Engineering, The University of Tokyo, Tokyo, Japan

⁴ Brigham and Women's Hospital and Harvard Medical School, Boston, USA

Abstract. We propose an optimization method for estimating patient-specific muscle fiber arrangement from clinical CT. Our approach first computes the structure tensor field to estimate local orientation, then a geometric template representing fiber arrangement is fitted using a B-spline deformation by maximizing fitness of the local orientation using a smoothness penalty. The initialization is computed with a previously proposed algorithm that takes account of only the muscle's surface shape. Evaluation was performed using a CT volume ($1.0 \text{ mm}^3/\text{voxel}$) and high resolution optical images of a serial cryo-section ($0.1 \text{ mm}^3/\text{voxel}$). The mean fiber distance error at the initialization of 6.00 mm was decreased to 2.78 mm after the proposed optimization for the gluteus maximus muscle, and from 5.28 mm to 3.09 mm for the gluteus medius muscle. The result from 20 patient CT images suggested that the proposed algorithm reconstructed an anatomically more plausible fiber arrangement than the previous method.

Keywords: Muscle fiber modeling · Fiber arrangement · Clinical CT

1 Introduction

Modeling of skeletal muscles has been investigated for biomechanical simulations in surgical planning, rehabilitation and sports medicine as well as for understanding of the detailed muscle anatomy from a general scientific interest [14]. The conventional string-type muscle model simplifying one muscle as a few strings has limitations in capturing the three-dimensional deformation which drastically alters the fiber arrangement that determines the force direction. Thus, patient-specific volumetric modeling has been drawing attention. The approaches to reconstructing patient-specific fiber arrangement are classified into two categories: (1) local orientation measurement inside the muscle

using medical images such as ultrasound (US) [15], diffusion tensor imaging (DTI) [12] and micro CT [11], and (2) computational modeling from the muscle’s outer shape using a template fitting approach [2], Laplacian vector field [3] and computational fluid dynamics [9]. Although these prior works successfully modeled fiber arrangement, their use in clinical routine is quite limited because the former approach has a limited field-of-measurement (e.g., US is mostly 2D, DTI requires long scan time resulting in motion artifact in a scan over the large area). The latter approach lacks the ability to represent patient-specific variation in fiber arrangement. On the other hand, we observed that a clinical CT (we use *clinical* to emphasize the contrast to *micro* CT) also has a potential to provide useful information regarding the muscle fiber arrangement (see Fig. 1 for comparison between a clinical CT and high resolution optical image in Visible Korean Human (VKH) dataset [8]). The muscle tissue and its surrounding connecting tissue exhibit slightly different x-ray attenuation coefficient (approximately 50–100 HU) which is visually enhanced in its projection view of the segmented muscle region. In this paper, we propose a method integrating the local orientation and global template approaches to allow an accurate patient-specific reconstruction using a modality common in clinical routine, i.e., CT. Our contributions are; (1) proposal of a muscle fiber modeling incorporating knowledge of the global fiber geometry into a noisy local orientation measurement from clinical CT, and (2) quantitative evaluation using tractography derived from a high resolution optical image and qualitative evaluation using 20 clinical CT images.

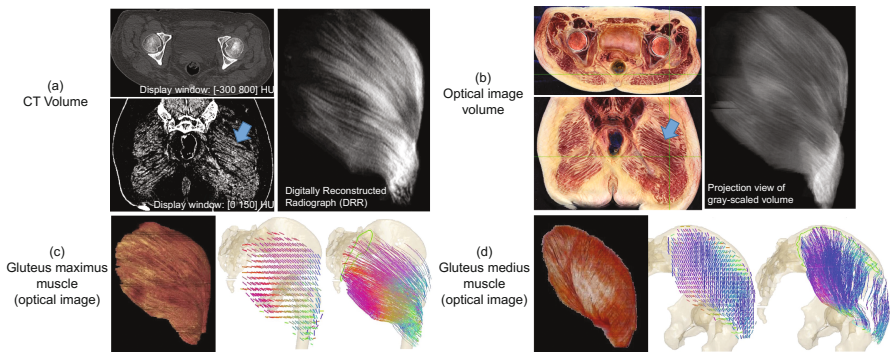


Fig. 1. Visible Korean Human dataset. (a, b) CT and optical image volumes with blue arrows indicating the corresponding muscle tissue. (c, d) Muscles used in the evaluation, (left) volume rendering of the optical image, (middle) local orientation at each voxel (color-mapped by the orientation), (right) tractography with fibers longer than 50 mm.

2 Method

2.1 Overview of the Proposed Method

Figure 2 shows an overview of the proposed method. First, the target muscle is segmented manually or using an automated algorithm proposed in [6], where the

hierarchical multi-atlas approach achieved an average surface error of 1.43 mm in 19 hip and thigh muscles. The optimization fits a B-spline interpolated geometric template representing the muscle’s fiber arrangement proposed by Blemker et al. [2] to a structure tensor field computed from CT, which represents orientation of neighborhood structure locally. The estimated B-spline grid provides the muscle fiber arrangement that best aligns with the orientation of the local structure at each voxel.

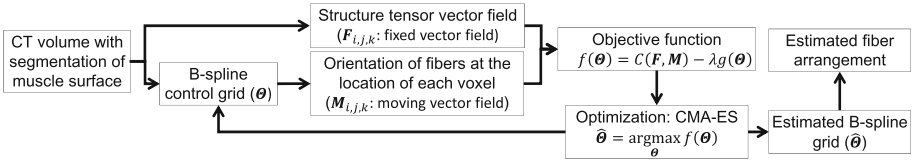


Fig. 2. Overview of the proposed method. The optimization minimizes the difference between two vector fields: (1) the least eigenvectors of the structure tensor from the CT volume, and (2) the vectors computed by the B-spline deformation (parameterized by θ) of a geometric template representing muscle fiber arrangement.

2.2 Computation of Structure Tensor Vector Field

We obtain the local orientation within the neighborhood at each voxel by computing the eigenvector corresponding to the smallest eigenvalue of the gradient-based structure tensor [1]. A Gaussian filter (with standard deviation of σ_1) was applied to the image before computing gradient to suppress noise and after computing the gradient (with std. of σ_2) to smooth the tensor field. $\sigma_1 = 1$ mm and $\sigma_2 = 5$ mm was used in the experiment below.

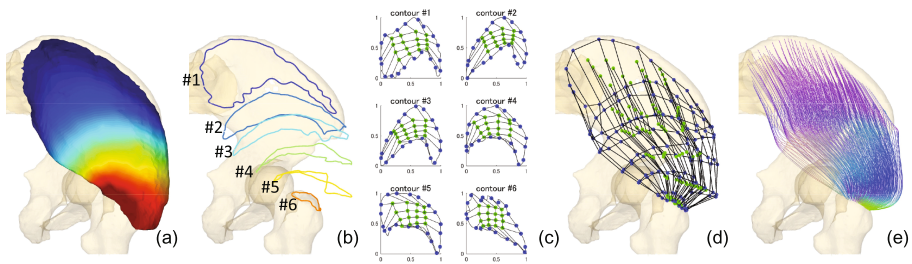


Fig. 3. Initialization of B-spline control grid. (a) Harmonic scalar field computed on the muscle’s surface vertices, (b) contours at iso-values in the scalar field, (c) initial rough grid fitting (blue: node on the contour, green: internal node), (d) initial B-spline control grid, (e) fiber arrangement template mapped by the control grid.

2.3 Initialization of B-Spline Grid

Figure 3 shows the steps to initialize the B-spline grid. The method follows the idea proposed by Kohout et al. [10], which computed the fiber arrangement from the muscle’s surface shape. First, the origin and insertion areas of the muscle are identified. While Kohout et al. identified these areas manually by an expert, we employ an automated method proposed in [6] which estimates the patient-specific muscle attachment areas based on the probabilistic atlas constructed with the physical measurements in cadavers. The method then computes the Harmonic scalar field [4] on the muscle surface (Fig. 3a) and its iso-lines provide a series of contours on the surface that smoothly connect origin and insertion and do not intersect each other (Fig. 3b). The contour is projected onto a plane fitted to the contour vertices. Then, a two-dimensional lattice grid is fitted to each projected contour (Fig. 3c). Those grid points are mapped back to the original space (Fig. 3d) and a geometric fiber template is deformed by this B-spline grid (Fig. 3e). Four types of geometric templates representing a fiber geometry of different types of muscles were proposed by Blemker et al. [2]. The template consists of a cluster of line-segments or curves connecting two boundary regions of a unit cube (see [2] for details). While we used only the “simple”-type template in this paper (the origin and insertion boundaries are simply connected by a cluster of straight lines), incorporation of other types of templates is straightforward by modifying the template.

2.4 Optimization of B-Spline Grid

Parameterization of Movement of B-Spline Nodes. We divide the nodes on each contour plane into two groups: the internal node and contour node (green and blue in Fig. 3c). The internal nodes move on the 2D contour plane, thus M_I internal nodes (green) were parameterized by $2M_I$ parameters. The contour nodes (blue) are constrained so that they always stay on the contour (1D curve) and maintain the order, thus the movement of the entire contour nodes on one contour was represented as one monotonic function that maps the 1D coordinate to the location on the contour. The monotonic function was parameterized by M_C parameters ($M_C = 6$ in this study). Thus, the number of parameters to optimize is $n(2M_I + M_C)$ in case for n contours (the appropriate n varies depending on the muscle).

Objective Function and Optimization. The objective function in the proposed optimization method is formulated as follows.

$$\hat{\Theta} = \arg \max_{\Theta} \left\{ Dice(\Omega_F, \Omega_M) \frac{1}{N} \sum_{\substack{i,j,k \in \\ \Omega_F \cap \Omega_M}} G(\theta_{i,j,k}(\Theta)); \sigma_{cost} \right\} + \lambda g(\Theta) \quad (1)$$

where $\theta_{i,j,k}$ is the angle between two vectors $\mathbf{F}_{i,j,k}$ (vector derived from structure tensor) and $\mathbf{M}_{i,j,k}(\Theta)$ (vector estimated by the current B-spline deformation parameterized by Θ), Ω_F and Ω_M are the regions covered by the fixed

and moving vector fields, N is the number of voxels in the region $\Omega_F \cap \Omega_M$, $G(A; \sigma)$ is Gaussian function with a standard deviation of σ , and $g(\Theta)$ represent the regularization term weighted by λ . In the experiment below, we employ the smoothness penalty common in B-spline deformation model using the total curvature. The first term in Eq. (1) represents degree of fitting between the estimated and target vector fields. Dice measure enforces the overlap between the two regions, which is 1.0 when two regions are completely overlapped, and Gaussian of the angle between the two vectors enforces alignment of the two vectors while ignoring outliers in the noisy structure tensor vector field.

CMA-ES (Covariance Matrix Adaptation Evolutionary Strategy) [7] is used as the optimizer. CMA-ES has been applied in a number of registration applications and known for its robustness against local optima, while it requires a large number of function evaluations. The optimization is performed in 3 levels in succession with decreasing σ_{cost} (40, 20, 10°) to gradually confine the inlier range and improve the fitting.

2.5 Evaluation Using the Ground Truth Dataset

To establish the ground truth for evaluation, we used the Visible Korean Human dataset [8] that includes the following two volumes (Fig. 1). (1) Optical image volume consisting of serially acquired photographs of cryo-section with a 0.1 mm³/voxel resolution. Segmentation masks of anatomical structures (e.g., muscles, bones, organs) are also available. (2) CT volume reconstructed with 1.0 mm³/voxel resolution. The slight deformation of the specimen exhibited between CT scanning and optical image scanning was corrected using a non-rigid image registration. The optical images were converted to gray-scale and structure tensor was computed with $\sigma_1 = 0.3$ mm and $\sigma_2 = 3$ mm. We applied tractography in 3D Slicer (www.slicer.org) [5] via the SlicerDMRI project (dmri.slicer.org) to the structure tensor field (Fig. 1c, d). The tractography applied to CT image did not produce fiber trajectories sufficient for evaluation due to the low signal-to-noise ratio in the structure tensor field.

In the following experiments, the error was evaluated using two metrics; (1) angular error at each voxel with the structure tensor field from optical image volume, and (2) fiber distance error defined as the mean distance between pairs of corresponding points on the fibers [13], which is often used in evaluation of white matter fibers, with the ground truth tractography.

3 Results

Figures 4 and 5 show the results of the proposed optimization with the gluteus maximus and medius muscles in the Visible Korean Human dataset. The optimization to the optical image was used as a reference to obtain the upper limit of the accuracy of the proposed method. In the gluteus maximus, both tensor vector angle error and fiber distance error were smaller than the previous method (i.e., initial estimate) after the proposed optimization. The accuracy

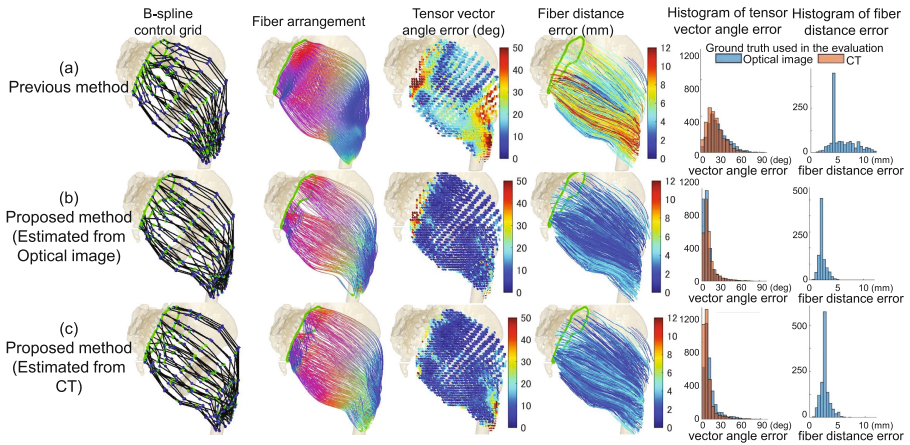


Fig. 4. Results with the gluteus maximus muscle of Visible Korean Human dataset. Results using (a) previous method [10], (b) proposed method with the optical image, (c) proposed method with CT. The second columns show fibers color-mapped according to the orientation of the local segment.

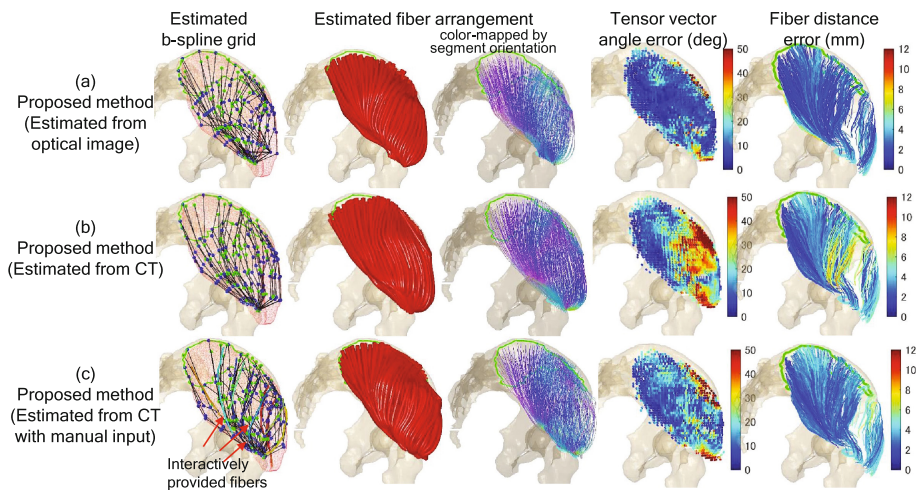


Fig. 5. Results with the gluteus medius muscle of Visible Korean Human dataset. Estimated from (a) optical image, (b) CT, and (c) CT with 11 interactively provided fibers shown in the left most column.

with CT image was almost the same as optical image, which can be attributed to the relatively thick fat tissue between the muscle tissue, resulting in sufficient contrast in CT to determine the fiber trajectory. On the other hand, the fat tissue in anterior region of the gluteus medius muscle is thin and does not have contrast in CT, resulting in low estimation accuracy as shown in 4th and

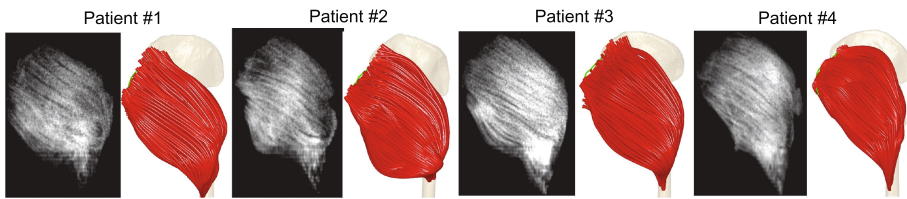


Fig. 6. Reconstruction of fiber arrangement from clinical CTs. Results of the gluteus maximus muscle of 4 (out of 20) example patients are shown.

5th columns in Fig. 5b. As a preliminary attempt, we tested if a small amount of user interaction improves the reconstruction accuracy. In DRR as in Fig. 1a, some of the fiber trajectories are visible, so we tried to provide those fiber lines interactively by an expert. The orientation of manually provided fibers were used in the cost function same as the image-derived structure tensor. The result in Fig. 5c demonstrated improved reconstruction accuracy by the user-provided 11 fiber lines. The mean fiber distance error of 6.00 mm with the previous method in the gluteus maximus decreased to 2.78 mm after the proposed optimization to CT, and from 5.28 mm to 3.09 mm in the gluteus medius without using the user-provided fibers. Figure 6 shows the reconstruction results on clinical CT of four example patients.

4 Discussion and Conclusion

We proposed a method to estimate patient-specific muscle fiber arrangement from clinical CT images. The experimental results suggested that the proposed method works accurately on the gluteus maximus muscle and posterior part of the gluteus medius muscle, but the anterior part exhibited lower accuracy, which was improved by few interactively provided fiber lines. Analysis of muscle fiber structure from clinical CT is especially beneficial for patient-specific biomechanical simulation in a clinical routine, because CT acquisition is stable (i.e., sensitivity of the acquired image to the scan environment is low) and can cover a large muscle quickly without the effect of motion artifact taking advantage of an increasing trend toward extremely low-dose scanning by an advancement of the detector technology and reconstruction algorithms, as opposed to MRI which requires a careful protocol design and is sensitive to the scan environment. One limitation of the current work concerns the demographic bias of the patient. Our clinical CTs tested in this study were obtained from a database of patients who were subjected to total hip arthroplasty surgery, where female accounts for a large fraction, thus all of our target images were female, which generally has more fat tissue between the muscle tissue which better facilitates determination of the fiber orientation. Nevertheless, this study showed a potential advantage in female patients with hip disorders where biomechanical simulation is especially valuable. Our future work includes further evaluation using cadaver specimens and a large-scale population analysis of *in vivo* skeletal muscle fiber arrangement.

Acknowledgement. This research was supported by MEXT/JSPS KAKENHI 26108004, JST PRESTO 20407, AMED/ETH the strategic Japanese-Swiss cooperative research program, NIH grant U01CA199459 and P41EB015902. The authors extend their appreciation to Prof. Min Suk Chung (Ajou University School of Medicine) for providing us the Visible Korean Human dataset.

References

1. Bigun, J.: Optimal orientation detection of linear symmetry. In: Proceedings of the IEEE First International Conference on Computer Vision, pp. 433–438 (1987)
2. Blemker, S.S., Delp, S.L.: Three-dimensional representation of complex muscle architectures and geometries. *Ann. Biomed. Eng.* **33**(5), 661–73 (2005)
3. Choi, H.F., Blemker, S.S.: Skeletal muscle fascicle arrangements can be reconstructed using a laplacian vector field simulation. *PLoS ONE* **8**(10), e77576 (2013)
4. Dong, S., Kircher, S., Garland, M.: Harmonic functions for quadrilateral remeshing of arbitrary manifolds. *Comput. Aided Geom. Des.* **22**(5), 392–423 (2005)
5. Fedorov, A., et al.: 3D slicer as an image computing platform for the quantitative imaging network. *Magn. Reson. Imaging* **30**(9), 1323–1341 (2012)
6. Fukuda, N., et al.: Estimation of attachment regions of hip muscles in CT image using muscle attachment probabilistic atlas constructed from measurements in eight cadavers. *Int. J. Comput. Assist. Radiol. Surg.* **12**, 1–10 (2017)
7. Hansen, N.: The CMA evolution strategy: a comparing review. In: Lozano, J.A., Larrañaga, P., Inza, I., Bengoetxea, E. (eds.) *Towards a New Evolutionary Computation. Studies in Fuzziness and Soft Computing*, vol. 192, pp. 75–102. Springer, Heidelberg (2006)
8. Jin, S., et al.: Visible Korean human: improved serially sectioned images of the entire body. *IEEE Trans. Med. Imaging* **24**(3), 352–360 (2005)
9. Joshua, I., et al.: Fiber tractography for finite-element modeling of transversely isotropic biological tissues of arbitrary shape using computational fluid dynamics. In: Proceedings of the Conference on Summer Computer Simulation, pp. 1–6 (2015)
10. Kohout, J., Kukaka, M.: Real-time modelling of fibrous muscle. *Comput. Graph. Forum* **33**(8), 1–15 (2014)
11. Kupczik, K., et al.: Reconstruction of muscle fascicle architecture from iodine-enhanced microct images: a combined texture mapping and streamline approach. *J. Theor. Biol.* **382**, 34–43 (2015)
12. Levin, D.I.W., et al.: Extracting skeletal muscle fiber fields from noisy diffusion tensor data. *Med. Image Anal.* **15**(3), 340–353 (2011)
13. O’Donnell, L.J., Westin, C.-F.: Automatic tractography segmentation using a high-dimensional white matter atlas. *IEEE Trans. Med. Imaging* **26**(11), 1562–1575 (2007)
14. Schenk, P., et al.: Determination of three-dimensional muscle architectures: validation of the dti-based fiber tractography method by manual digitization. *J. Anat.* **223**(1), 61–68 (2013)
15. Zhou, Y., et al.: Estimation of muscle fiber orientation in ultrasound images using revolving hough transform (RVHT). *Ultrasound Med. Biol.* **34**(9), 1474–81 (2008)